Atherosclerosis 286 (2019) 60–70

Contents lists available at ScienceDirect

Atherosclerosis

journal homepage: www.elsevier.com/locate/atherosclerosis

Naringenin enhances the regression of atherosclerosis induced by a chow diet in *Ldlr*$^{-/-}$ mice

Amy C. Burke[a,b], Brian G. Sutherland[a], Dawn E. Telford[a,c], Marisa R. Morrow[a], Cynthia G. Sawyez[a,c], Jane Y. Edwards[a,c], Murray W. Huff[a,b,c,*]

[a] Molecular Medicine, Robarts Research Institute, The University of Western Ontario, 1151 Richmond St N., London, Ontario, N6A 5B7, Canada
[b] Department of Biochemistry, The University of Western Ontario, 1151 Richmond St N., London, Ontario, N6A 5B7, Canada
[c] Department of Medicine, The University of Western Ontario, 1151 Richmond St N., London, Ontario, N6A 5B7, Canada

HIGHLIGHTS

- Intervention by naringenin plus chow in *Ldlr*$^{-/-}$ mice enhances atherosclerosis regression; smaller lesions, fewer macrophages.
- Naringenin plus chow reduces circulating monocytes and bone marrow myelopoietic progenitor cells, contributing to regression.
- Naringenin plus chow enhances correction of hyperlipidemia, obesity, fatty liver and insulin resistance, compared to chow only.

Keywords:
Atherosclerosis
Regression
Mouse studies
Flavonoid
Intervention

ABSTRACT

Background and aims: Naringenin is a citrus-derived flavonoid with lipid-lowering and insulin-sensitizing effects leading to athero-protection in *Ldlr*$^{-/-}$ mice fed a high-fat diet. However, the ability of naringenin to promote atherosclerosis regression is unknown. In the present study, we assessed the capacity of naringenin to enhance regression in *Ldlr*$^{-/-}$ mice with diet-induced intermediate atherosclerosis intervened with a chow diet.

Methods: Male *Ldlr*$^{-/-}$ mice were fed a high-fat, cholesterol-containing (HFHC) diet for 12 weeks to induce intermediate atherosclerosis and metabolic dysfunction. Subsequently, a group of these mice were sacrificed for baseline analyses and the remainder either 1) continued on the HFHC diet, 2) switched to a chow diet or 3) switched to chow diet supplemented with naringenin.

Results: After 12 weeks induction, intermediate lesions developed in the aortic sinus. Intervention with chow alone slowed lesion growth, while intervention with naringenin-supplemented chow completely halted lesion growth. Lesions were characterized by features of improved morphology. Compared to chow alone, naringenin reduced plaque macrophages and modestly increased smooth muscle cells. Investigating processes that contributed to improved plaque morphology, we showed naringenin further reduced plasma triglycerides and cholesterol compared to chow alone. Furthermore, elevated monocytosis and myelopoiesis were further corrected by intervention with naringenin compared to chow alone. Metabolically, naringenin enhanced the correction of insulin resistance, hepatic steatosis and obesity compared to chow alone, potentially contributing to enhanced regression.

Conclusions: Naringenin supplementation to chow enhances atherosclerosis regression in male *Ldlr*$^{-/-}$ mice. These studies further underscore the potential therapeutic utility of naringenin.

1. Introduction

Atherosclerosis is a progressive, lipid and inflammatory-driven disease characterized by the growth of fatty plaques within the arterial wall [1]. It is the major underlying cause of myocardial infarction and stroke, thereby contributing to cardiovascular disease being the most

Abbreviations: BM, bone marrow; CE, cholesteryl ester; CMP, common myeloid progenitor cell; FC, free cholesterol; FPLC, fast protein liquid chromatography; GMP, granulocyte and macrophage progenitor cell; HBSS, Hank's buffered salt solution; HFHC, high-fat, cholesterol-containing; HOMA-IR, homeostasis model assessment of insulin resistance; HSPC, hematopoietic stem and progenitor cell; MEP, megakaryocyte and erythrocyte progenitor cell; MPC, myeloid progenitor cell; Nar, naringenin; NEFA, non-esterified fatty acid; OCT, optimal cutting temperature

* Corresponding author. Robarts Research Institute, Rm 4222, The University of Western Ontario, 1151 Richmond St. N., London, Ontario, N6A 5B7, Canada.
E-mail address: mhuff@uwo.ca (M.W. Huff).

https://doi.org/10.1016/j.atherosclerosis.2019.05.009
Received 26 January 2019; Received in revised form 31 March 2019; Accepted 8 May 2019
Available online 09 May 2019

common cause of morbidity and mortality in western society [2]. Most patients present without symptoms during the majority of disease progression, resulting in administration of treatment after extensive disease is established [2]. Despite many promising therapeutic studies in animal models, there is often a lack of translatability into humans.

The majority of pre-clinical cardiovascular therapeutic studies have been conducted in progression or prevention mouse models, whereby the therapeutic is added at the same time as the disease initiator, the high-fat diet [3,4]. Efficacy has been measured as the ability of a gene knockout or therapeutic to prevent or slow atherosclerosis, compared to the pro-atherogenic control. Recently, clinically-relevant models have been developed to study cardiovascular drugs in intervention models to assess atherosclerosis regression [3,5–7]. These mouse models have established atherosclerosis prior to treatment, similar to humans starting a therapy or treatment. In this way, the ability of interventions to regress or reverse disease can be evaluated.

Epidemiological evidence suggests an inverse correlation between the consumption of flavonoids, a class of plant-derived polyphenols, and cardiovascular disease [8]. Naringenin is a grapefruit-derived flavonoid that has lipid-lowering and insulin-sensitizing properties [9,10]. Previous prevention studies in *Ldlr*$^{-/-}$ mice show that naringenin attenuates obesity, insulin resistance, hyperlipidemia, hepatic steatosis and atherosclerosis [11–14]. When investigated in an intervention model, naringenin supplemented to a high-fat diet completely corrected many metabolic indices including obesity, adipose tissue accumulation and inflammation, and glucose tolerance [15]. However, naringenin did not completely correct hyperlipidemia, hepatic steatosis, or insulin intolerance, leading to improvement in atherosclerotic lesion morphology, but not lesion regression [15]. With the exception of one report [16], mouse studies that have achieved lesion regression required transfer to a low fat, cholesterol-free diet (usually chow) together with a genetic manipulation to amplify plasma lipid lowering [5,17,18].

In the present study, we assessed the ability of naringenin to enhance regression of diet-induced atherosclerosis in *Ldlr*$^{-/-}$ mice, in which the intervention consisted of a chow diet. Addition of naringenin to chow completely halted atherosclerotic plaque growth and significantly improved plaque composition compared to intervention with chow alone. Plaque morphological improvements were accompanied by reduced circulating blood monocytes and reduced bone marrow myelopoietic progenitor populations in naringenin-treated mice. Metabolically, naringenin enhanced the correction of hyperlipidemia, insulin intolerance and obesity compared to intervention with chow alone, contributing to atherosclerosis regression in this model.

2. Materials and methods

2.1. Animals and diets

Male *Ldlr*$^{-/-}$ mice on a C57BL/6 background (Jackson Laboratory, Bar Harbor, MA) were housed in pairs in standard cages at 23 °C on a 12 h light and 12 h dark cycle. Male mice were used because they develop a stronger diet-induced metabolic syndrome phenotype than do female mice [19], thereby increasing the likelihood of achieving reversal of metabolic dysregulation with an intervention, using a reasonable sample size. Future studies in female mice will require a larger sample size. Mice (10–12 weeks of age, n = 40; 10/group) were fed *ad libitum* a high-fat, cholesterol containing diet (HFHC) (42% of calories from fat, 0.2% cholesterol, Teklad TD09268, Envigo, Madison WI) for 12 weeks. One subgroup of these mice was sacrificed to provide baseline data (n = 10). Remaining mice were divided amongst 3 groups. For the subsequent 12 weeks, one group remained on the HFHC diet (n = 10), one group switched to isoflavone-free standard rodent chow (12% of calories from fat, Teklad Global 16% Protein Rodent Diet 2016, Envigo) (n = 10), and one group switched to the same chow supplemented with 3% (wt/wt) naringenin (#N5893, Millipore-Sigma) (n = 10). This dose (3.6 g/kg/d) was based on dose-response experiments in prior mouse prevention studies [13] and is required due to the limited bioavailability of naringenin (3–6%) in mice. The equivalent dose for humans was calculated to be 0.3 g/kg/d [20]. Food intake was measured daily, and body weight measured weekly. Caloric intake was calculated as weight of food eaten (g/day) corrected for caloric content (chow: 3.0 kcal/g; HFHC: 4.5 kcal/g). Experimental procedures were approved by the Animal Care Committee at the University of Western Ontario (protocol # AUP-2016-057).

2.2. Blood and tissue collection

Mice were fasted for 6 h at the start of the light cycle prior to sacrifice. At sacrifice, animals were anesthetized with Ketamine-Xylazine (100 µg/g Ketamine hydrochloride, Bioniche Animal Health Canada Inc., Belleville, ON and 10 µg/g Xylazine, Bayer Healthcare, Animal Health Division, Bayer Inc., Toronto ON). Tissue dissections were performed *via* midline incision. Blood was collected *via* cardiac puncture in syringes containing 80 µL of 7% Na_2-EDTA, and plasma separated by centrifugation. To dissect the heart, the left ventricle was perfused with phosphate buffered saline containing heparin (10 units/mL) and the right atrium cut to drain the perfusate. The heart, full-length aorta and liver were dissected and prepared for analyses as described previously [15,21,22].

2.3. Glucose tolerance and insulin tolerance tests

A glucose tolerance test was performed following a 6 h fast by *i. p.* injection with 15% glucose in 0.9% NaCl (1 g/kg body weight) [13]. An insulin tolerance test was conducted following a 5 h fast by *i. p.* injection with insulin (0.6 IU/kg body weight; Novolin GE Toronto, Novo Nordsik, Cooksville, ON) [13]. Homeostasis model assessment of insulin resistance (HOMA-IR) for mice was calculated as: HOMA-IR = 26 x fasting insulin level (ng/mL) x fasting glucose level (mg/dL)/405 [23].

2.4. Tissue lipids

Lipids from liver and full-length aortae dissected free of fat and connective tissue were extracted as described previously [22]. [Cholesteryl-1,2–^{3}H(N)]Cholesteryl oleate (PerkinElmer, Guelph, Canada: #NET746L) was added to assess recovery. Solvent extracts were dried under N_2 and re-solubilized in 1% Triton X-100 in chloroform prior to analysis with enzymatic reagents (Roche Diagnostics and WAKO Diagnostics) [22].

2.5. Plasma measurements

Plasma triglyceride and total cholesterol were measured on a Cobas Mira S autoanalyzer (Roche Diagnostics, Laval, Canada) using calibrators and controls from Roche Diagnostics. Enzymatic reagents for triglyceride (Roche Diagnostics: triglycerides/glycerol blanked #11877771 216) and cholesterol (Roche Diagnostics: Cholesterol CHOD-PAP #11491458-216) were used. Fresh-EDTA plasma (50 µL) was separated by Fast Protein Liquid Chromatography (FPLC) using an AKTA purifier and a Superose 6 column as previously described [22]. Blood glucose was measured in whole blood (Bayer Contour Blood Glucose Monitoring System) [13]. Plasma insulin was determined in frozen EDTA-plasma samples by mouse-specific ELISA (ALPCO Diagnostics, Salem, NH: mouse ultrasensitive ELISA #80-INSMSU-E01) [22]. Plasma non-esterified fatty acids (NEFAs) were determined enzymatically (Wako Chemicals HR Series NEFA-HR (2) #999–34691, VWR, Mississauga, Canada).

2.6. Tissue histology and immunohistochemistry

Histological and morphometric analyses were performed as described previously [15,21,22]. Frozen livers were sectioned at 8 µm

using a Leica CM 3050S cryostat. Liver sections were stained with Oil Red-O (ORO, Sigma-Aldrich) and visualized using brightfield microscopy. Frozen serial sections of the aortic sinus from hearts frozen in OCT (70–100 per heart, 10 μm), initiating anterior to the origin of the aortic valves, were prepared using a Leica CM 3050S cryostat. For quantitation of lesion area in the aortic sinus, sections were stained with ORO. For quantitation of necrotic core size in plaques, aortic sinus sections were stained with H&E. Acellular areas were measured (no nuclei, little eosin-staining), and areas greater than 3000 μm^2 were considered necrotic core. Immunohistochemistry staining for macrophages by CD68, smooth muscle α-actin and activated caspase-3, was performed as described previously (Online Table) [15,21,22]. Photomicrographs were obtained using an Olympus BX50 microscope and a QImaging Retiga EXi FAST camera. Collagen fibrils were assessed using circular polarizing microscopy on aortic sinus sections stained with picrosirius red (Polysciences, Warrington, PA) [21,22].

2.7. Flow cytometry

Blood and bone marrow cell analyses were performed in a separate experiment in male *Ldlr*$^{-/-}$ mice (n = 10/group) using the same induction and intervention protocol described above.

Blood leukocytes: Monocytes and neutrophils were identified from whole blood as previously described [15,24]. For each mouse sample, 100 μL of blood was used. Cells were stained with a cocktail of antibodies against CD45-eFluor®450, Ly6-C/G-PerCP-Cy™5.5 and CD115-APC on ice for 20 min in the dark (Online Table) similar to previous studies [15,24]. Red blood cells were lysed in 1X PharmLyse (BD Biosciences, Cedarlane) for 13 min at room temperature. The stained white blood cells were centrifuged, washed, and resuspended in flow-buffer (Hank's buffered salt solution (HBSS) + 0.1% BSA, w/v) and fixed with 4% paraformaldehyde. Monocytes were identified as CD45^{hi} CD115^{hi} and further identified into Ly6-C^{hi} and Ly6-C^{lo}; neutrophils were identified as CD45^{hi} CD115^{lo} Ly6-C/G^{hi} (Gr-1).

Hematopoietic stem cells: Hematopoietic stem and progenitor cells (HSPCs) from the bone marrow were analyzed by flow cytometry. Bone marrow was harvested from femurs and tibias, and red blood cells lysed as previously described [15]. Cells were re-suspended in 1 mL flow-buffer and blocked with normal goat serum. Cells were centrifuged at 500 *g* for 5 min at 6 °C, and the supernatant aspirated. Bone marrow was resuspended in 4 mL of flow-buffer. For each bone marrow sample, 150 μL of suspension was used. Cells were stained with a cocktail of antibodies against FITC Mouse Hematopoietic Lineage Cocktail (CD3 (17A2), CD45R (B220) (RA3-6B2), CD11b (M1/70), TER-119, Ly-G6 (Gr-1) (RB6-8C5)), Brilliant Violet 421™ Anti-mouse CD117 (c-Kit), Brilliant Violet 605™ anti-mouse Ly-6A/E (Sca-1), Alexa Fluor®700 Anti-mouse CD16/32 and PE Anti-mouse CD34 on ice for 20 min in the dark (Supplementary Table) similar to previous studies [15,24]. The stained white blood cells were centrifuged, washed, and resuspended in flow-buffer and fixed with 4% paraformaldehyde. HSPCs were identified as Lin$^-$, Sca-1$^+$ and ckit$^+$ (LSK) while the hematopoietic progenitor subsets were separated using antibodies to CD16/32 (FcγRII/III) and CD34. CMPs were identified as lin$^-$, Sca-1$^-$, ckit$^+$, CD34^{hi}, FcγRII/III^{lo}, GMPs as lin$^-$, Sca-1$^-$, ckit$^+$, CD34^{hi}, FcγRII/III^{hi}, MEPs as lin$^-$, Sca-1$^-$, ckit$^+$, CD34^{lo}, FcγRII/III^{lo}.

Flow cytometry was performed using an LSRII (for analysis) running FACS DiVa software. All flow cytometry data were analyzed using FlowJo software (Tree Star Inc.)

2.8. Gene expression

RNA was isolated from aliquots of liver and reverse transcription performed as previously described [15,22]. mRNA abundances were measured by quantitative real-time PCR on an ABI ViiA 7 Sequence Detection System (ABI) according to the manufacturer's instructions as previously described [15,22]. Expression levels for each gene were normalized to *Gapdh* expression. All primer and probe sets were purchased as TaqMan Assays (ABI).

2.9. Statistical analysis

Data is presented as mean ± SEM. Data were initially tested for normal distribution using the Shapiro-Wilk test and equal variance by *F* test. If the data were normally distributed, a 1-way ANOVA was performed followed by a Tukey post hoc test using GraphPad Prism 7. Significance thresholds were $p \leq 0.05$. Significant differences are indicated by different lowercase letters. If the data were not normally distributed, the nonparametric Kruskal-Wallis 1-way ANOVA on ranks was performed, followed by a Tukey post hoc test. Significance thresholds were $p \leq 0.05$. Significant differences are indicated by uppercase letters.

3. Results

3.1. Naringenin enhances lipid lowering observed with chow intervention

In the present study, the impact of naringenin on atherosclerosis regression was assessed in the setting of low plasma lipids in *Ldlr*$^{-/-}$ mice. Baseline metrics were measured after 12 weeks on the HFHC diet. For the subsequent 12 weeks, remaining mice either continued on the HFHC diet, or switched to an intervention diet of isoflavone-free standard chow supplemented with or without 3% (wt/wt) naringenin. From baseline, continuation on the HFHC diet maintained increased plasma cholesterol and triglycerides, whereas intervention with chow reduced plasma cholesterol and triglyceride levels (Fig. 1). Intervention with naringenin supplemented chow potentiated the reduction in plasma cholesterol (−83.2% vs −76.6%) and triglycerides (−79.4% vs −65.6%) (Fig. 1). FPLC separation of plasma lipoproteins revealed that naringenin plus chow decreased VLDL-cholesterol, LDL-cholesterol and VLDL-triglycerides to a greater extent than chow alone (Fig. 1).

3.2. Naringenin completely halts atherosclerosis

To evaluate atherosclerosis regression, aortic lipids and plaque size in the aortic sinus were measured. Unlike continuation on the HFHC diet, intervention with chow slowed the accumulation of aortic free and esterified cholesterol (Fig. 2A and B). Intervention with naringenin plus chow further slowed the accumulation of aortic cholesterol (Fig. 2A and B) and reduced aortic triglycerides compared to all other treatment groups (Fig. 2C). To investigate this further, lesion size in the aortic sinus was quantitated (Fig. 2D). Induction with the HFHC diet promoted intermediate lesion development and continuation on the HFHC diet further increased lesion size more than 2-fold (Fig. 2D). Intervention with chow alone slowed lesion growth 66%, whereas the addition of naringenin to chow completely halted lesion growth (−92%) (Fig. 2D).

3.3. Naringenin improves aortic sinus atherosclerosis lesion pathology

Macrophages comprise the majority of cells within early to intermediate atherosclerotic lesions, consistent with observations in HFHC-induced plaques at baseline (Fig. 3A and B). Continuation on the HFHC diet reduced the contribution of macrophages to lesion cellularity (−33%) as the size and complexity of lesions increased (Fig. 3A and B). Chow intervention significantly reduced macrophage content from baseline (−63%). This reduction was augmented (−75%) by the addition of naringenin (Fig. 3A and B). To further characterize plaques, features of stability, including smooth muscle α-actin, acting as a marker of smooth muscle cells (SMC), as well as collagen content, were assessed (Fig. 3A–D). SMCs in sinus lesions at baseline were ~4.2% of total plaque area (Fig. 3A and C). Continuation of the HFHC diet decreased SMCs to ~2% of plaque area (Fig. 3A and C). While

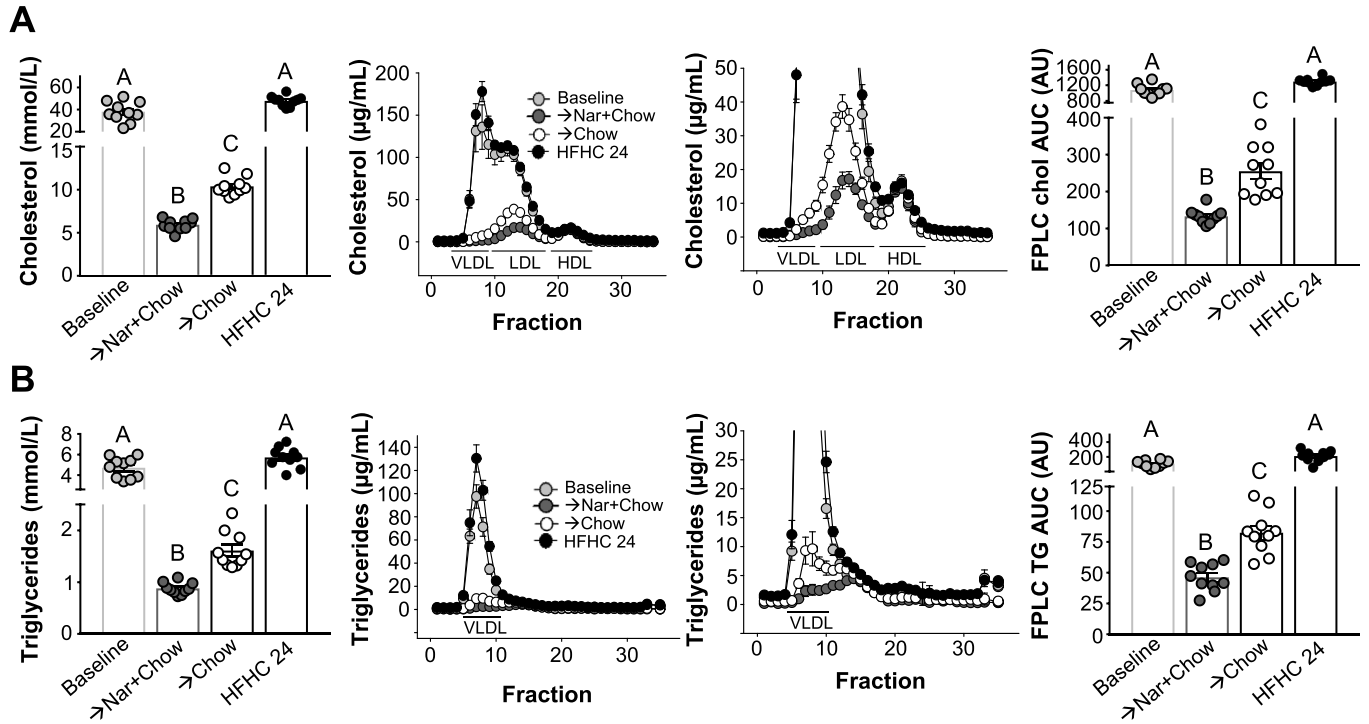

Fig. 1. Naringenin supplementation enhances the reduction in plasma lipids.
Male *Ldlr*$^{-/-}$ mice were fed a HFHC diet for 12 weeks (Baseline) followed by a 12-week intervention with chow or chow plus 3% naringenin (Nar). Plasma lipids were measured at 12 and 24 weeks. (A) Total plasma cholesterol, FPLC-separated plasma cholesterol (full and enlarged profile) and VLDL-plus LDL-cholesterol area under the FPLC curve (AUC) (n = 10/group). (B) Plasma triglycerides, FPLC-separated plasma triglycerides (full and enlarged profile) and VLDL-triglyceride AUC (n = 10/group). FPLC fractions, VLDL: 5–10, LDL: 11–19, HDL: 20–26. Data represent the mean ± SEM. Different uppercase letters indicate statistical difference by Kruskal-Wallis 1-way ANOVA with post-hoc Tukey test ($p < 0.05$).

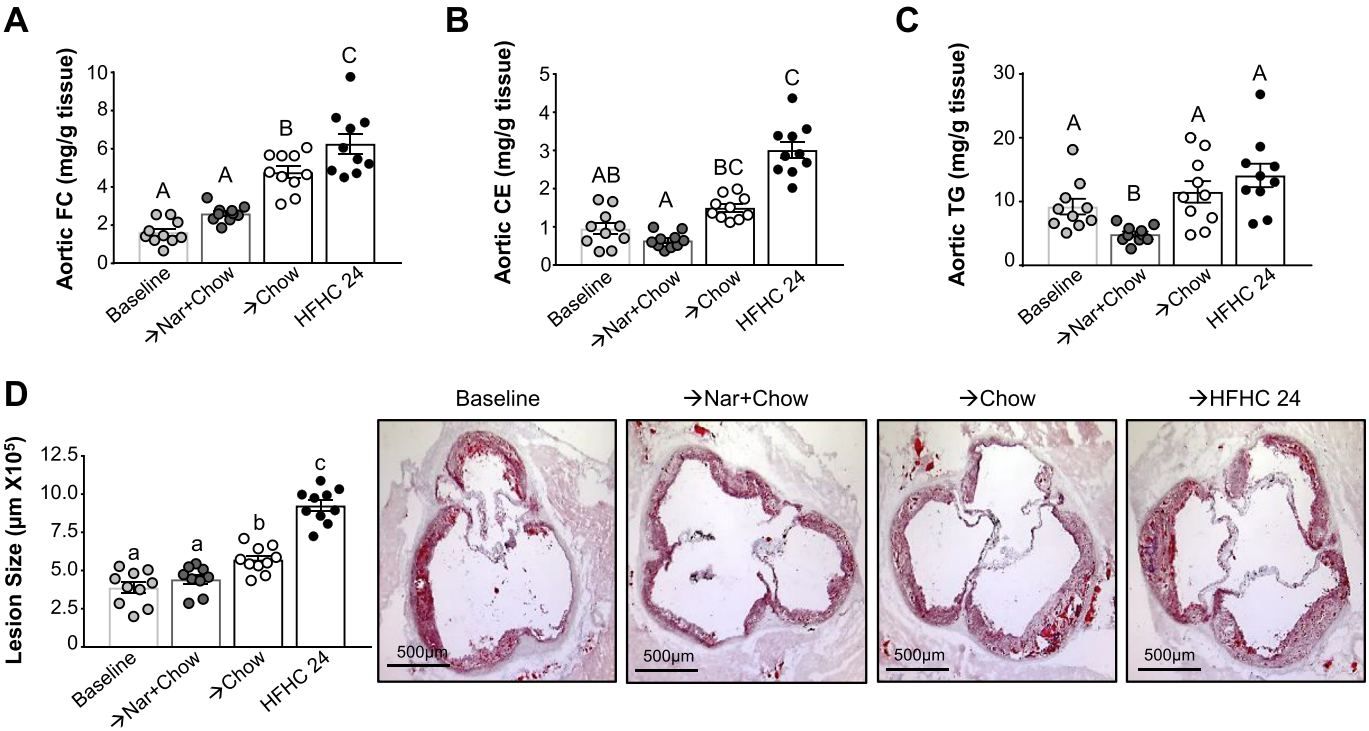

Fig. 2. Naringenin supplementation completely halts atherosclerotic lesion growth.
Male *Ldlr*$^{-/-}$ mice were fed a HFHC diet for 12 weeks (Baseline) followed by a 12-week intervention with chow or chow plus 3% naringenin (Nar). Aortic sinus sections were assessed histologically, and aortae were dissected free from fat and lipids analyzed. (A) Aortic free cholesterol (FC; n = 10/group). (B) Aortic cholesteryl ester (CE; n = 10/group). (C) Aortic triglycerides (TGs; n = 9-10/group). (D) Lesion area in the aortic root and representative sections stained with oil-red O and counterstained with hematoxylin (n = 9-10/group). Data represent the mean ± SEM. Different lowercase letters indicate statistical difference by ANOVA with post-hoc Tukey test ($p < 0.05$). Different uppercase letters indicate statistical difference by Kruskal-Wallis 1-way ANOVA with post-hoc Tukey test ($p < 0.05$).

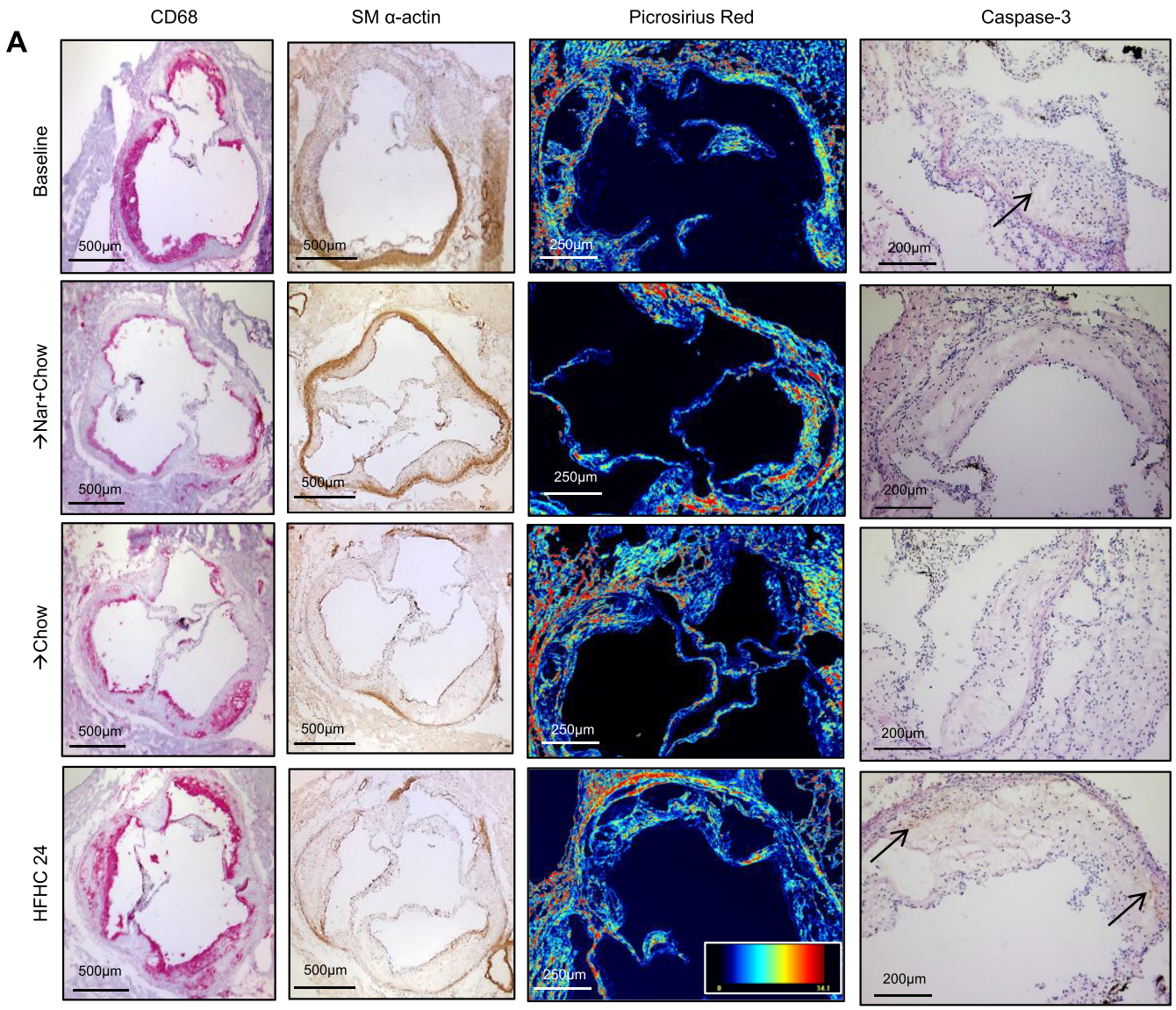

(caption on next page)

Fig. 3. Naringenin supplementation improves atherosclerotic plaque morphology.
Male *Ldlr*$^{-/-}$ mice were fed a HFHC diet for 12 weeks (Baseline) followed by a 12-week intervention with chow or chow plus 3% naringenin (Nar). Aortic sinus sections were assessed histologically. (A) Representative sections for each stain in the aortic sinus. (B) Percent of lesion area occupied by CD68^{+} macrophages (n = 7-10/group). (C) Percent of lesion area occupied by smooth muscle (SM) α-actin (n = 10/group). (D) Percent of lesion occupied by collagen (n = 9-10/group). (E) Mean collagen retardation (nm) in lesions (n = 10/group). (F) Percent of lesion positive for activated caspase-3 (n = 8-10/group). (G) Percent of lesion comprised of necrotic core (n = 9-10/group). Data represent the mean ± SEM. Different lowercase letters indicate statistical difference by ANOVA with post-hoc Tukey test ($p < 0.05$). Different uppercase letters indicate statistical difference by Kruskal-Wallis 1-way ANOVA with post-hoc Tukey test ($p < 0.05$). *N.S* indicates non-significance.

intervention with chow alone slowed the reduction in SMC content (~3% of plaque area), intervention with naringenin plus chow appeared to halt the reduction in lesion SMCs (~4% of plaque area) (Fig. 3A and C). Collagen content tends to increase with lesion complexity as evidenced by the increase in collagen content and organization in mice continuing on HFHC (Fig. 3A,D and E). Intervention with chow alone or chow plus naringenin increased collagen content and organization from baseline, which were modestly higher compared to mice remaining on the HFHC diet (Fig. 3A,D and E). Analyses of necrotic core size and apoptotic cell accumulation, both markers of advanced plaques, revealed that both parameters were increased from baseline in mice continuing on the HFHC diet, although increases in necrotic core were not significant (Fig. 3A, F and G). Intervention with both chow alone or chow plus naringenin reversed apoptotic cell accumulation and tended to slow necrotic core growth to a similar extent, suggesting improved lesion morphology (Fig. 3A, F and G).

3.4. Naringenin reduces blood monocytes

Studies have demonstrated that reduced monocyte recruitment into plaques contributes to reduced macrophage content and enhanced regression [18]. HFHC-feeding for 24 weeks maintained blood leukocyte levels similar to baseline levels (Fig. 4A–E). In contrast, intervention with chow alone reduced both neutrophils (−18%) and total monocytes (−36%) from baseline, with a greater reduction in Ly6C^{hi} monocytes compared to Ly6C^{lo} monocytes (Fig. 4A–E). Intervention with naringenin plus chow reduced neutrophils a further 19% and total monocytes a further 38%, with the further reduction in Ly6C^{hi} monocytes (−62%) being of greater magnitude than the further reduction in Ly6C^{lo} monocytes (−12%) (Fig. 4A–E).

3.5. Naringenin reduces bone marrow progenitor proliferation

The magnitude reduction in circulating peripheral blood mononuclear cells with naringenin plus chow intervention suggested suppression of bone marrow progenitor cell proliferation. Consistent with previous studies, HSPCs were elevated in the bone marrow of *Ldlr*$^{-/-}$ mice during induction with the HFHC diet (Fig. 4F; Supplementary Fig. IA) [24]. Intervention with chow alone reduced HSPCs 33% from baseline (Fig. 4F; Supplementary Fig. IA). With naringenin plus chow, the extent of reduction was modestly enhanced (trend), reducing HSPCs (−37%) from baseline (Fig. 4F; Supplementary Fig. IA). This suggests that reduced bone marrow myelopoiesis may contribute to reduced circulating monocytes with both intervention diets. To examine further along the differentiation lineage, bone marrow myeloid progenitor cells (MPCs) were assessed (Fig. 4G; Supplementary Fig. IA). A similar trend emerged with reduced bone marrow MPCs with chow intervention (−17%) and a slight enhancement (trend) of reduction with naringenin plus chow (Fig. 4G). Assessment of the common myeloid progenitor (CMP) and granulocyte macrophage progenitor (GMP) populations with both interventions, showed a trend towards reduction in CMPs but no effect was observed for GMPs (Fig. 4H and I; Supplementary Fig. IB). There was no effect on erythrocyte progenitor pools (MEPs) (Fig. 4J; Supplementary Fig. IB).

3.6. Naringenin enhances insulin sensitivity

Insulin resistance in mice has been correlated with worsening atherosclerosis and enhanced monocytosis and myelopoiesis [25]. The HFHC diet induced hyperinsulinemia and impaired insulin tolerance at baseline (Fig. 5A and B). Continuation on the HFHC diet maintained hyperinsulinemia and a suppressed insulin tolerance test response (Fig. 5A and B). Intervention with chow decreased hyperinsulinemia 38%, while naringenin plus chow reduced hyperinsulinemia 85% (Fig. 5A). Insulin tolerance was unaffected by intervention with chow alone, however naringenin plus chow enhanced glucose clearance in response to insulin by 38% (Fig. 5B). Assessment of glucose homeostasis in HFHC-fed *Ldlr*$^{-/-}$ mice confirmed the development of a moderate hyperglycemia, which persisted with continuation of HFHC diet (Fig. 5C). Compared to baseline, intervention with chow alone did not affect fasting blood glucose levels, whereas intervention with naringenin significantly reduced fasting blood glucose by 38% (Fig. 5C). To assess if changes in hyperinsulinemia were reflected by alterations in glucose homeostasis, glucose tolerance tests were performed (Fig. 5D). At baseline, glucose tolerance was impaired and continuation on the HFHC diet or intervention with chow alone had no further effect on glucose clearance after a glucose challenge (Fig. 5D). In contrast, supplementation of naringenin to chow significantly enhanced glucose tolerance (Fig. 5D). Furthermore, HOMA-IR calculations showed that intervention with naringenin plus chow reduced HOMA-IR to a greater extent than intervention with chow alone (Fig. 5E). Plasma non-esterified fatty acids were reduced similarly by chow and by naringenin plus chow (Fig. 5F).

3.7. Naringenin improves liver lipids and body weight

Metabolic disturbances contribute to atherosclerosis in mice and their resolution has been linked to lesion regression [3]. Hepatic triglycerides and cholesterol were increased at baseline and remained elevated with continuation of the HFHC diet (Fig. 6A–C). Liver sections were characterized by the accumulation of large lipid droplets (Fig. 6C). Intervention with chow alone completely reversed hepatic lipid accumulation (Fig. 6A–C). Naringenin plus chow enhanced the reduction in triglycerides (−75% vs −68%) (Fig. 6A) and cholesteryl ester (−93.1% vs −89.9%, trend) (Fig. 6B), whereas the reductions in free cholesterol (−40%) were similar to those with chow alone (Fig. 6B). Lipid droplets in liver sections appeared smaller with intervention by naringenin plus chow, compared to intervention with chow alone (Fig. 6C). The greater reduction in hepatic lipids was associated with increased expression of genes linked to enhanced mobilization and oxidation of fatty acids. Naringenin plus chow increased the mRNA of *Pnpla2* (1.73-fold), *Cpt1a* (1.24-fold) and *Pgc1a* (1.88-fold) compared to chow alone, suggesting augmented fatty acid oxidation (Fig. 6D–F).

Mice rapidly gained weight during the 12-week HFHC induction phase, which continued in HFHC-fed mice throughout the subsequent 12 weeks (Fig. 6G). Intervention with chow alone promoted rapid weight loss over the first 6 weeks, which plateaued for the last 6 weeks of intervention (Fig. 6G). Similarly, naringenin plus chow induced rapid weight loss in the first 6 weeks, followed by a plateau, although body weights at sacrifice were 20% lower compared to chow alone; however, this was not significant (Fig. 6G). Assessment of epididymal adiposity

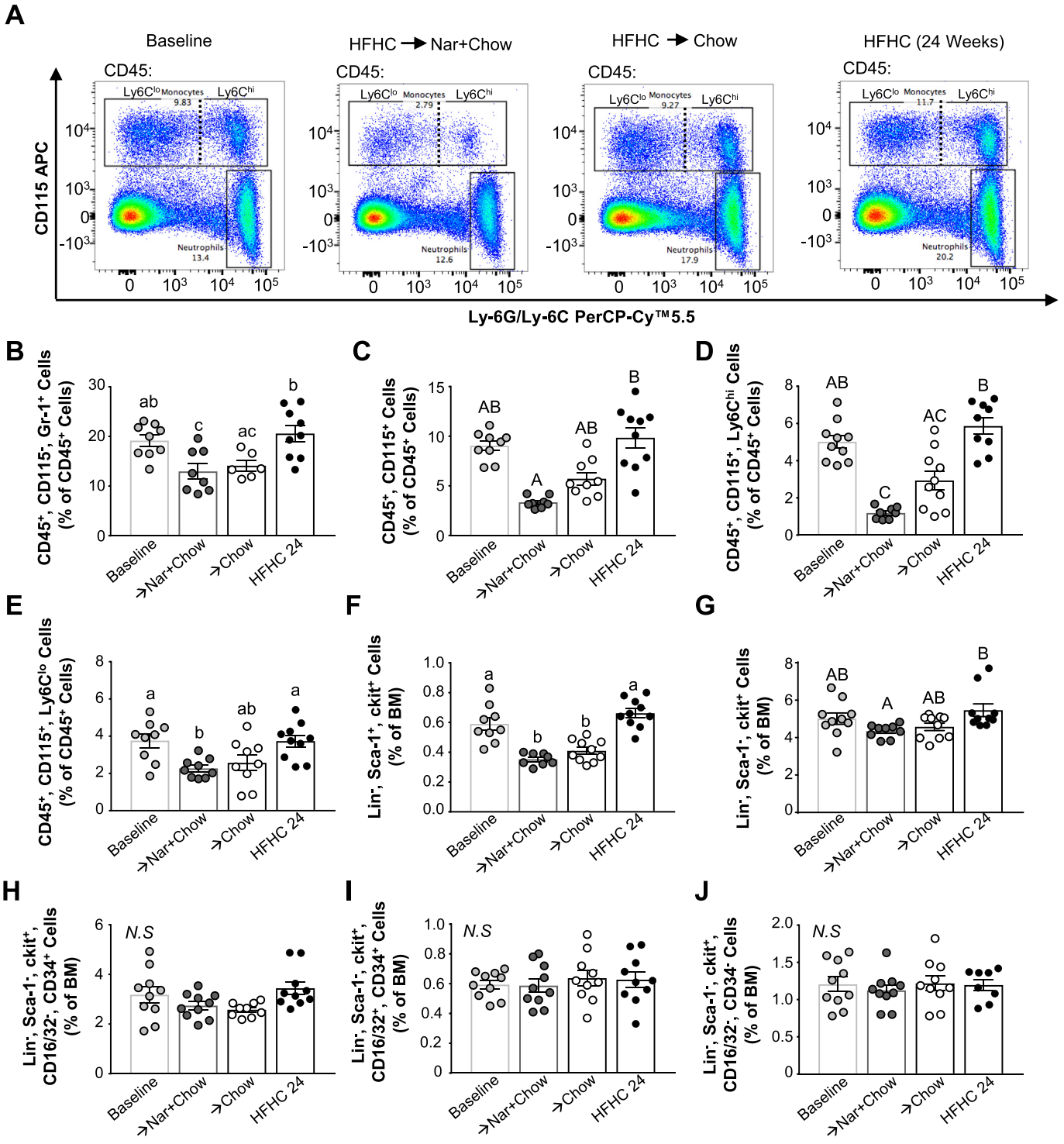

Fig. 4. Naringenin supplementation reduces blood monocytes.
Male *Ldlr*$^{-/-}$ mice were fed a HFHC diet for 12 weeks (Baseline) followed by a 12-week intervention with chow or chow plus 3% naringenin (Nar). Blood and bone marrow cells were isolated, stained and analyzed by flow cytometry. (A) Representative pseudocolor plots depicting gating of peripheral blood mononuclear cells (PBMCs). Percent of PBMCs that are: (B) neutrophils (n = 6-9/group), or (C) monocytes (n = 9-10/group). Percent of PBMCs that are: (D) Ly6C^{hi} monocytes (n = 8-10/group), or (E) Ly6C^{lo} monocytes (n = 9-10/group). Percent of bone marrow (BM) cells that are: (F) hematopoietic stem and progenitor cells (HSPCs; n = 8-10/group), (G) myeloid progenitor cells (MPCs; n = 9-10/group), (H) common myeloid progenitor cells (CMPs; n = 9-10/group), (I) granulocyte and macrophage progenitor cells (GMPs; n = 10/group) or (J) megakaryocyte and erythrocyte progenitor cells (MEPs; n = 8-10/group). Data represent the mean ± SEM. Different lowercase letters indicate statistical difference by ANOVA with post-hoc Tukey test ($p < 0.05$). Different uppercase letters indicate statistical difference by Kruskal-Wallis 1-way ANOVA with post-hoc Tukey test ($p < 0.05$). *N.S* indicates non-significance.

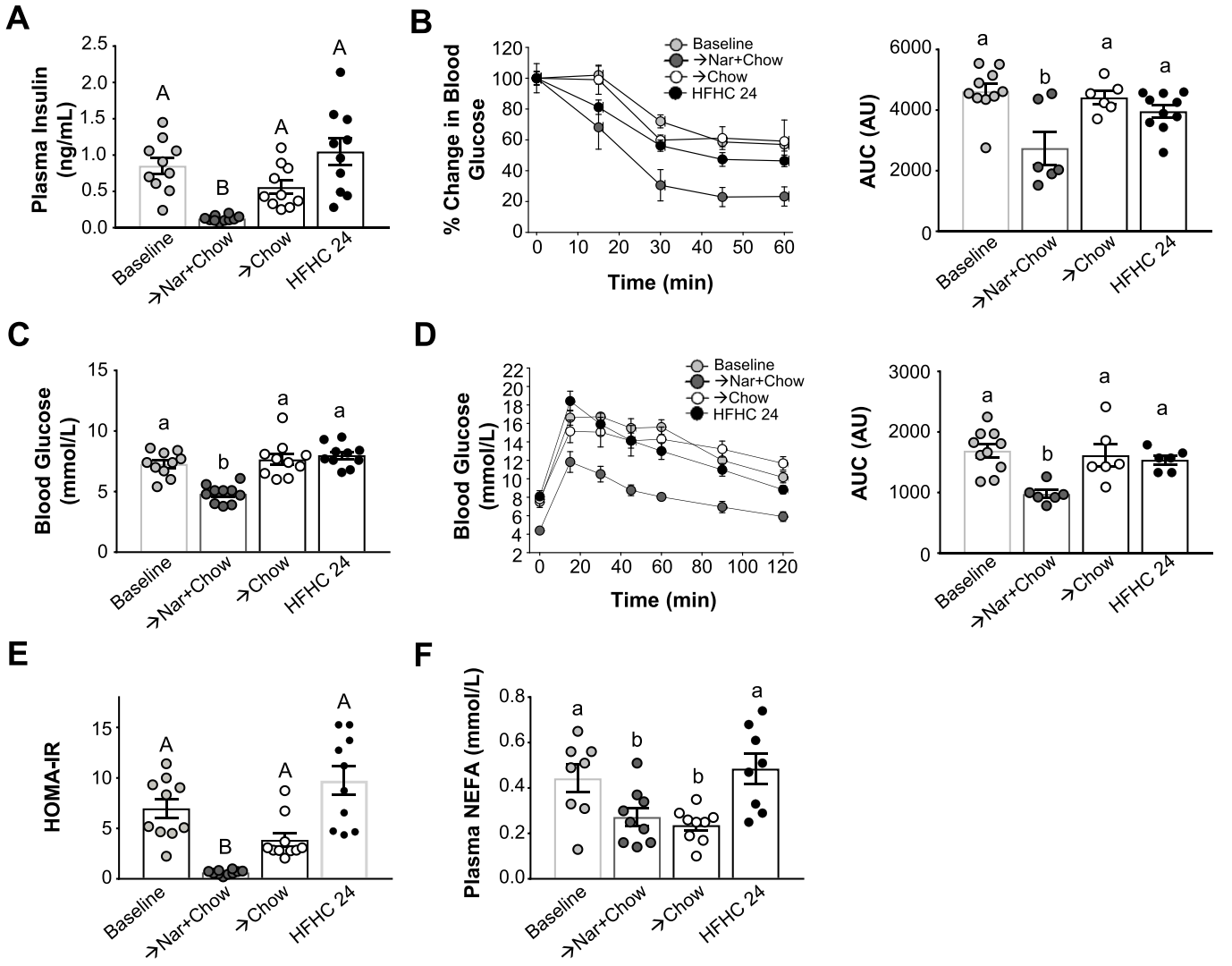

Fig. 5. Naringenin supplementation enhances insulin sensitivity.
Male *Ldlr*$^{-/-}$ mice were fed a HFHC diet for 12 weeks (Baseline) followed by a 12-week intervention with chow or chow plus 3% naringenin (Nar). (A) Plasma insulin levels (n = 10/group). (B) Insulin tolerance test as a percent of baseline glucose (n = 6-10/group). (C) Fasting blood glucose levels (n = 10/group). (D) Glucose tolerance test (n = 6-10/group). (E) Homeostasis model assessment of insulin resistance (HOMA-IR; n = 10/group). (F) Plasma non-esterified fatty acids (NEFAs; n = 8-9/group). Data represent the mean ± SEM. Different lowercase letters indicate statistical difference by ANOVA with post-hoc Tukey test ($p < 0.05$). Different uppercase letters indicate statistical difference by Kruskal-Wallis 1-way ANOVA with post-hoc Tukey test ($p < 0.05$).

showed that the modest enhancement in weight loss by naringenin was due to a significant reduction in adiposity compared to chow alone (Fig. 6H). Importantly, during the intervention phase, caloric intake was similar between all groups (Fig. 6I).

4. Discussion

Regression of atherosclerosis has become an important clinical objective and therefore, studies of the underlying mechanisms and therapeutics that induce atherosclerosis regression have become increasingly relevant. In the majority of published mouse regression studies, intervention involves genetic modulation, whereas regression studies with novel therapeutics are limited [3]. The data presented herein demonstrates that in *Ldlr*$^{-/-}$ mice with established diet-induced atherosclerosis, intervention with the citrus flavonoid naringenin enhances regression of atherosclerosis compared to intervention with a chow diet alone. The growth in size of aortic sinus plaques was completely halted and plaques were characterized by a significant reduction in macrophages, attenuation in the reduction of smooth muscle cells and similar amounts of collagen, apoptotic cells and necrotic core sizes. Together, this suggests improved lesion morphology. Naringenin intervention amplified the reduction in circulating monocytes, due to an attenuation of myelopoiesis in the bone marrow. Furthermore, enhanced atherosclerosis regression in naringenin-treated mice was primarily driven by a greater reduction in plasma cholesterol along with improved insulin resistance and adiposity.

The most well characterized cell type in atherosclerosis regression is the macrophage [3,26]. Similar to a number of other regression studies, we observed reduced macrophage content within plaques of naringenin-treated mice. Macrophages tended to be located at the luminal periphery of the plaque, consistent with other intervention studies in mice [5,7,18]. Monocyte dynamics are intrinsically involved in atherosclerosis regression, including reduced recruitment of monocytes from the circulation, egress of macrophages out of the plaque or attenuated proliferation within the plaque [3]. In this study, naringenin intervention decreased circulating monocytes (Ly6C^{hi} and Ly6C^{lo}), which was accompanied by a reduction in bone marrow progenitor populations. Furthermore, chow intervention decreased circulating neutrophils, which was slightly enhanced by the addition of naringenin. Reduced circulating neutrophils may decrease their recruitment into lesions,

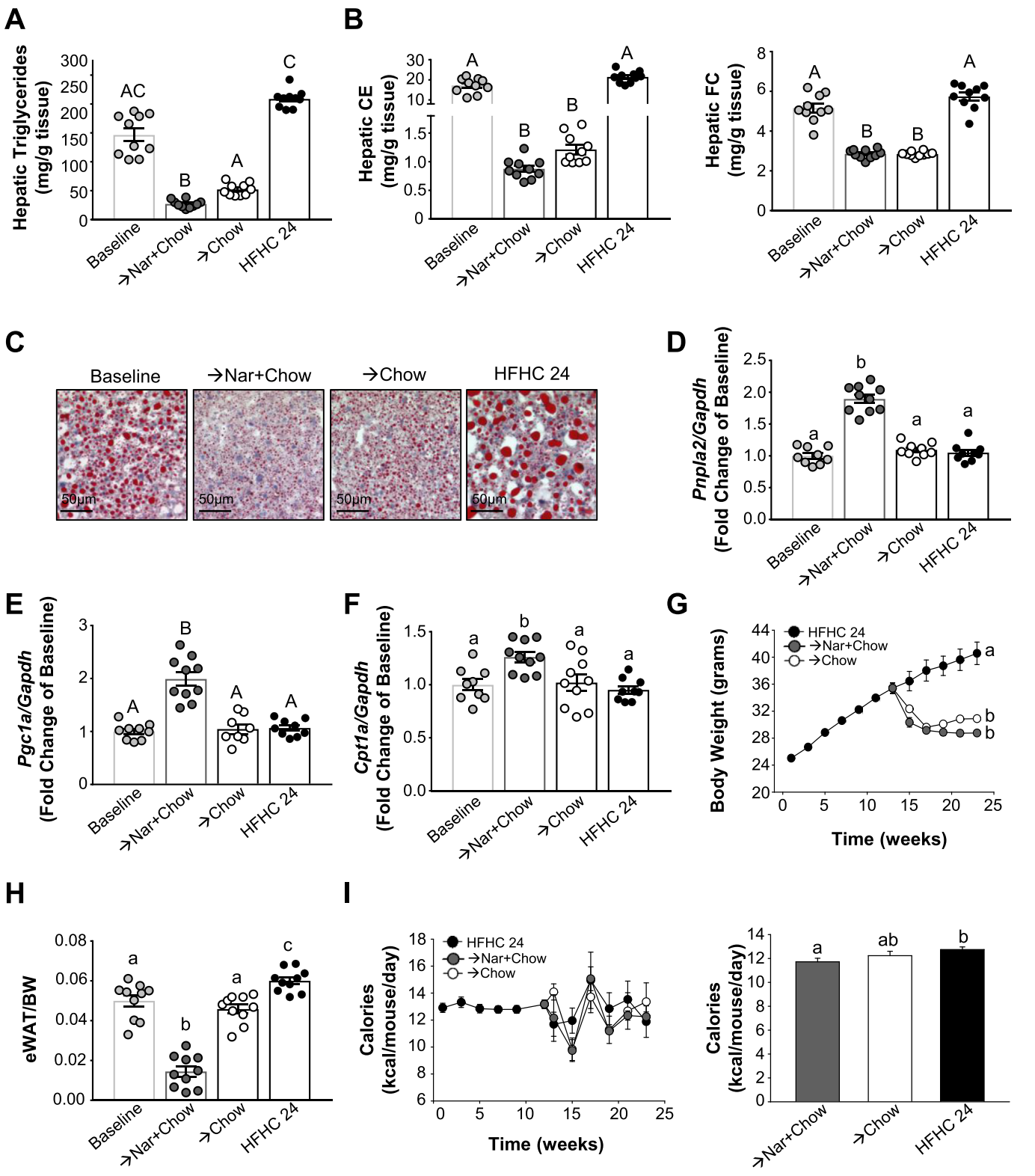

Fig. 6. Naringenin supplementation enhances weight loss.
Male *Ldlr*$^{-/-}$ mice were fed a HFHC diet for 12 weeks (Baseline) followed by a 12 week-intervention with chow or chow plus 3% naringenin (Nar). (A) Hepatic triglyceride (n = 8-10/group) and (B) hepatic cholesteryl ester and free cholesterol (n = 8-10/group). (C) Representative liver sections stained with oil red-O. D-F; Hepatic expression of (D) *Pnpla2,* (E) *Pgc1a and* (F) *Cpt1a* expressed as a fold change of baseline (n = 8-10/group). (G) Body weight (n = 10/group). H; Epididymal fat pad weight/total body weight (n = 10/group). (I) Daily caloric intake and average caloric intake (n = 5/group). Data represent the mean ± SEM. Different lowercase letters indicate statistical difference by ANOVA with post-hoc Tukey test ($p < 0.05$). Different uppercase letters indicate statistical difference by Kruskal-Wallis 1-way ANOVA with post-hoc Tukey test ($p < 0.05$).

attenuate monocyte recruitment and slow lesion development through reduced neutrophil trap formation [27]. Similar results have been observed in the context of reversed hyperlipidemia, obesity and hyperglycemia [24,28,29], suggesting that the enhanced reduction of plasma atherogenic lipoproteins and other metabolic improvements with naringenin treatment attenuated myelopoiesis, thereby contributing to atherosclerosis regression. However, we cannot exclude a direct effect of naringenin on myelopoiesis. Although the reversal of hyperlipidemia, hyperglycemia or adiposity with naringenin intervention likely resulted in a reduction in the recruitment of circulating monocytes to the regressing plaque, we did not perform trafficking studies to confirm the contribution of monocyte recruitment, proliferation or macrophages egress to the suppression of lesion macrophages.

Some of the morphological changes in the plaque during regression involve other cell types. Enhanced SMC content and increased collagen content and organization is associated with a stable fibrous cap [21,30,31]. Although both interventions appeared to stabilize lesion SMC content, which trended to be more effective with naringenin, this did not correlate with an increase in collagen content or organization, as observed previously in studies of atherosclerosis regression in mice [21,30–32]. It is possible that naringenin intervention prevented loss of smooth muscle α-actin expression, known to occur during the transition of SMCs into foam cells [33,34], but these SMCs retained their inability to lay down collagen matrix in the milieu of more advanced lesions [35]. Thus, it would be important in future studies to determine the origin of smooth muscle α-actin expressing cells during regression, which could be determined using lineage-tracing [36]. Necrotic core size is an important indicator of plaque stability [1]. In the present study, necrotic core growth was halted to a similar extent with both naringenin plus chow and chow alone interventions. Additionally, both interventions reduced the accumulation of apoptotic cells in the plaque. During regression, macrophage phenotype is known to shift towards M2, which is more efficient at efferocytosis, or the clearance of apoptotic cells [21,37,38]. Although we did not examine macrophage phenotype, it is possible that naringenin polarized macrophages towards an M2 phenotype. Furthermore, enhanced or improved efferocytosis, as well as inhibition of apoptosis, could contribute to reduced apoptotic cell accumulation within lesions and halt the growth of the necrotic core [38].

Naringenin enhanced the reversal of obesity, insulin insensitivity, hepatic steatosis and hyperlipidemia, all factors that could contribute to atherosclerosis regression [5,28,29]. However, we could not exclude additional contributions from direct effects of naringenin on plaque cells. Previous mouse intervention studies administered treatments that directly targeted lesions, without effect on plasma lipids or metabolic indices [31,39]. It is possible that naringenin has pleiotropic effects on lesional cells aside from its metabolic effects. Experiments in cell culture have demonstrated that naringenin treatment of vascular SMCs reduced proliferation and migration *via* heme oxygenase-1 [40] and in THP-1 macrophages, naringenin enhanced the expression of genes involved in cholesterol efflux via LXRα [41]. Context-dependently, both these effects could enhance lesion regression. Future experiments could address these pleiotropic effects by evaluating the ability of naringenin to regress lesions in *Apoe*$^{-/-}$ mice, which can develop atherosclerosis spontaneously on a chow-based diet or in *Apoe*$^{-/-}$ mice fed a high-fat diet, which do not develop as severe metabolic dysfunction as in the high-fat fed *Ldlr*$^{-/-}$ model [42,43]. Prevention studies in *Apoe*$^{-/-}$ mice fed a semi-synthetic diet demonstrated that naringin, the glycosylated form of naringenin, at 0.02% had no effect on lesion development [43]. With a naringin dose 10-fold lower than that of naringenin used in the present study, it is difficult to conclude whether pleiotropic effects were lacking or if the dose used was insufficient to elicit them.

The mechanism(s) through which naringenin regulates lipid metabolism, adiposity and insulin sensitivity are not completely understood. Previous *in vitro* studies demonstrated that naringenin activated insulin signaling independent of the insulin receptor or insulin receptor substrate [9] and does not activate PPARα, PPARδ or PPARγ [13]. In mice, naringenin upregulated hepatic fatty acid oxidation, independent of peroxisomal proliferation [13]. The upstream mechanism(s) governing these effects have remained somewhat elusive. Metabolic protection by naringenin does not require fibroblast growth factor 21. Although Fgf21 elicits similar metabolic improvements as naringenin when given exogenously to mice, naringenin treatment of high fat diet-fed *Fgf21*$^{-/-}$ mice prevented metabolic dysfunction and obesity as effectively as in wildtype mice [14]. Short-term treatment of *Ob/Ob* mice with naringenin corrected hyperlipidemia and insulin insensitivity, and decreased body weight [14], suggesting that the effect of naringenin intervention was independent of leptin deficiency. Treatment of weight cycling C57BL6/J mice with the combination of apigenin and naringenin increased brown adipose tissue *Ucp1* expression [44]. However, in *Ldlr*$^{-/-}$ mice intervened with naringenin on a HFHC diet, there was no effect on brown adipose tissue *Ucp1* or other genes linked to browning [15]. Metabolic protection by the flavonoid nobiletin has been associated with enhanced amplitude of circadian rhythms, specifically in obese mice [45], however the effect of naringenin at the doses used in the present study have not been examined.

In conclusion, intervention with naringenin supplemented to chow in male *Ldlr*$^{-/-}$ mice enhanced atherosclerosis regression compared to intervention with chow alone. Lesions were characterized by reduced macrophages and improved morphology, due in part to reduced circulating monocytes and myelopoiesis in the bone marrow, which were primarily determined by enhanced improvements in hyperlipidemia and other metabolic indices. These studies highlight the potential therapeutic utility of the citrus flavonoid, naringenin, especially in the context of existing atherosclerosis.

Conflicts of interest

The authors declared they do not have anything to disclose regarding conflict of interest with respect to this manuscript.

Financial support

This work was supported by grants from the Heart and Stroke Foundation of Canada (G-14-0006179) and Canadian Institutes of Health Research (MOP-126045) to MWH. ACB was supported by a Canadian Diabetes Association Doctoral Research Award (DS-3-14-4588-AB).

Author contributions

A.C.B. generated the data and wrote the manuscript. B.G.S., D.E.T., M.R.M., C.G.S., and J.Y.E. generated data and reviewed the manuscript. M.W.H. oversaw the project and helped write the manuscript.

Acknowledgements

The authors would like to thank Kristin Chadwick (London Regional Flow Cytometry Facility) and Corby Fink (Robarts Research Institute) for assistance in designing flow cytometry staining panels and technical assistance, and Julia St. John for technical assistance in flow cytometry experiments.

Appendix A. Supplementary data

Supplementary data to this article can be found online at https://doi.org/10.1016/j.atherosclerosis.2019.05.009.

References

[1] K.J. Moore, I. Tabas, Macrophages in the pathogenesis of atherosclerosis, Cell 145

(2011) 341–355.
[2] A.S. Go, D. Mozaffarian, V.L. Roger, et al., Heart disease and stroke statistics–2014 update: a report from the American Heart Association, Circulation 129 (2014) e28–e292.
[3] A.C. Burke, M.W. Huff, Regression of atherosclerosis: lessons learned from genetically modified mouse models, Curr. Opin. Lipidol. 29 (2018) 87–94.
[4] C.A. Gleissner, Translational atherosclerosis research: from experimental models to coronary artery disease in humans, Atherosclerosis 248 (2016) 110–116.
[5] J.E. Feig, S. Parathath, J.X. Rong, et al., Reversal of hyperlipidemia with a genetic switch favorably affects the content and inflammatory state of macrophages in atherosclerotic plaques, Circulation 123 (2011) 989–998.
[6] B. Hewing, S. Parathath, C.K. Mai, et al., Rapid regression of atherosclerosis with MTP inhibitor treatment, Atherosclerosis 227 (2013) 125–129.
[7] K.J. Rayner, F.J. Sheedy, C.C. Esau, et al., Antagonism of miR-33 in mice promotes reverse cholesterol transport and regression of atherosclerosis, J. Clin. Investig. 121 (2011) 2921–2931.
[8] E.E. Mulvihill, A.C. Burke, M.W. Huff, Citrus flavonoids as regulators of lipoprotein metabolism and atherosclerosis, Annu. Rev. Nutr. 36 (2016) 275–299.
[9] E.M. Allister, N.M. Borradaile, J.Y. Edwards, et al., Inhibition of microsomal triglyceride transfer protein expression and apolipoprotein B100 secretion by the citrus flavonoid naringenin and by insulin involves activation of the mitogen-activated protein kinase pathway in hepatocytes, Diabetes 54 (2005) 1676–1683.
[10] N.M. Borradaile, L.E. de Dreu, M.W. Huff, Inhibition of net HepG2 cell apolipoprotein B secretion by the citrus flavonoid naringenin involves activation of phosphatidylinositol 3-kinase, independent of insulin receptor substrate-1 phosphorylation, Diabetes 52 (2003) 2554–2561.
[11] E.E. Mulvihill, J.M. Assini, B.G. Sutherland, et al., Naringenin decreases progression of atherosclerosis by improving dyslipidemia in high-fat-fed low-density lipoprotein receptor-null mice, Arterioscler. Thromb. Vasc. Biol. 30 (2010) 742–748.
[12] J.M. Assini, E.E. Mulvihill, B.G. Sutherland, et al., Naringenin prevents cholesterol-induced systemic inflammation, metabolic dysregulation, and atherosclerosis in *Ldlr-/-* mice, J. Lipid Res. 54 (2013) 711–724.
[13] E.E. Mulvihill, E.M. Allister, B.G. Sutherland, et al., Naringenin prevents dyslipidemia, apolipoprotein B overproduction, and hyperinsulinemia in LDL receptor-null mice with diet-induced insulin resistance, Diabetes 58 (2009) 2198–2210.
[14] J.M. Assini, E.E. Mulvihill, A.C. Burke, et al., Naringenin prevents obesity, hepatic steatosis, and glucose intolerance in male mice independent of fibroblast growth factor 21, Endocrinology 156 (2015) 2087–2102.
[15] A.C. Burke, B.G. Sutherland, D.E. Telford, et al., Intervention with citrus flavonoids reverses obesity, and improves metabolic syndrome and atherosclerosis in obese *Ldlr-/-* mice, J. Lipid Res. 59 (2018) 1714–1728.
[16] S. Zimmer, A. Grebe, S.S. Bakke, et al., Cyclodextrin promotes atherosclerosis regression via macrophage reprogramming, Sci. Transl. Med. 8 (2016) 333ra350.
[17] D. Basu, Y. Hu, L.A. Huggins, et al., Novel reversible model of atherosclerosis and regression using oligonucleotide regulation of the LDL receptor, Circ. Res. 122 (2018) 560–567.
[18] S. Potteaux, E.L. Gautier, S.B. Hutchison, et al., Suppressed monocyte recruitment drives macrophage removal from atherosclerotic plaques of *Apoe-/-* mice during disease regression, J. Clin. Investig. 121 (2011) 2025–2036.
[19] J.E. Kanter, F. Kramer, S. Barnhart, et al., A novel strategy to prevent advanced atherosclerosis and lower blood glucose in a mouse model of metabolic syndrome, Diabetes 67 (2018) 946–959.
[20] S. Reagan-Shaw, M. Nihal, N. Ahmad, Dose translation from animal to human studies revisited, FASEB J. 22 (2008) 659–661.
[21] L.A. Bojic, A.C. Burke, S.S. Chhoker, et al., Peroxisome proliferator-activated receptor delta agonist GW1516 attenuates diet-induced aortic inflammation, insulin resistance, and atherosclerosis in low-density lipoprotein receptor knockout mice, Arterioscler. Thromb. Vasc. Biol. 34 (2014) 52–60.
[22] J.P. Samsoondar, A.C. Burke, B.G. Sutherland, et al., Prevention of diet-Induced metabolic dysregulation, inflammation, and atherosclerosis in *Ldlr-/-* mice by treatment with the ATP-citrate lyase inhibitor bempedoic acid, Arterioscler. Thromb. Vasc. Biol. 37 (2017) 647–656.
[23] N. Murakami, T. Ohtsubo, Y. Kansui, et al., Mice heterozygous for the xanthine oxidoreductase gene facilitate lipid accumulation in adipocytes, Arterioscler. Thromb. Vasc. Biol. 34 (2014) 44–51.
[24] A.J. Murphy, M. Akhtari, S. Tolani, et al., ApoE regulates hematopoietic stem cell proliferation, monocytosis, and monocyte accumulation in atherosclerotic lesions in mice, J. Clin. Investig. 121 (2011) 4138–4149.
[25] K.E. Bornfeldt, I. Tabas, Insulin resistance, hyperglycemia, and atherosclerosis, Cell Metabol. 14 (2011) 575–585.
[26] M. Peled, E.A. Fisher, Dynamic aspects of macrophage polarization during atherosclerosis progression and regression, Front. Immunol. 5 (2014) 579.
[27] Y. Doring, M. Drechsler, O. Soehnlein, et al., Neutrophils in atherosclerosis: from mice to man, Arterioscler. Thromb. Vasc. Biol. 35 (2015) 288–295.
[28] P.R. Nagareddy, A.J. Murphy, R.A. Stirzaker, et al., Hyperglycemia promotes myelopoiesis and impairs the resolution of atherosclerosis, Cell Metabol. 17 (2013) 695–708.
[29] P.R. Nagareddy, M. Kraakman, S.L. Masters, et al., Adipose tissue macrophages promote myelopoiesis and monocytosis in obesity, Cell Metabol. 19 (2014) 821–835.
[30] A.C. Foks, G.H. van Puijvelde, I. Bot, et al., Interruption of the OX40-OX40 ligand pathway in LDL receptor-deficient mice causes regression of atherosclerosis, J. Immunol. 191 (2013) 4573–4580.
[31] A. Huang, T.L. Young, V.T. Dang, et al., 4-phenylbutyrate and valproate treatment attenuates the progression of atherosclerosis and stabilizes existing plaques, Atherosclerosis 266 (2017) 103–112.
[32] F. Willecke, C. Yuan, K. Oka, et al., Effects of high fat feeding and diabetes on regression of atherosclerosis induced by low-density lipoprotein receptor gene therapy in LDL receptor-deficient mice, PLoS One 10 (2015) e0128996.
[33] N.A. Pidkovka, O.A. Cherepanova, T. Yoshida, et al., Oxidized phospholipids induce phenotypic switching of vascular smooth muscle cells in vivo and in vitro, Circ. Res. 101 (2007) 792–801.
[34] D. Gomez, G.K. Owens, Smooth muscle cell phenotypic switching in atherosclerosis, Cardiovasc. Res. 95 (2012) 156–164.
[35] M.J. Frontini, C. O'Neil, C. Sawyez, et al., Lipid incorporation inhibits Src-dependent assembly of fibronectin and type I collagen by vascular smooth muscle cells, Circ. Res. 104 (2009) 832–841.
[36] L.S. Shankman, D. Gomez, O.A. Cherepanova, et al., KLF4-dependent phenotypic modulation of smooth muscle cells has a key role in atherosclerotic plaque pathogenesis, Nat. Med. 21 (2015) 628–637.
[37] J.E. Feig, J.X. Rong, R. Shamir, et al., HDL promotes rapid atherosclerosis regression in mice and alters inflammatory properties of plaque monocyte-derived cells, Proc. Natl. Acad. Sci. U.S.A. 108 (2011) 7166–7171.
[38] E.A. Van Vre, H. Ait-Oufella, A. Tedgui, et al., Apoptotic cell death and efferocytosis in atherosclerosis, Arterioscler. Thromb. Vasc. Biol. 32 (2012) 887–893.
[39] J. Tang, M.E. Lobatto, L. Hassing, et al., Inhibiting macrophage proliferation suppresses atherosclerotic plaque inflammation, Sci. Adv. 1 (2015).
[40] S. Chen, Y. Ding, W. Tao, et al., Naringenin inhibits TNF-alpha induced VSMC proliferation and migration via induction of HO-1, Food Chem. Toxicol. 50 (2012) 3025–3031.
[41] J. Saenz, C. Santa-Maria, M.E. Reyes-Quiroz, et al., Grapefruit flavonoid naringenin regulates the expression of LXRalpha in THP-1 macrophages by modulating AMP-activated protein kinase, Mol. Pharm. 15 (2018) 1735–1745.
[42] G.S. Getz, C.A. Reardon, Do the *Apoe-/-* and *Ldlr-/-* mice yield the same insight on atherogenesis? Arterioscler. Thromb. Vasc. Biol. 36 (2016) 1734–1741.
[43] A. Chanet, D. Milenkovic, C. Deval, et al., Naringin, the major grapefruit flavonoid, specifically affects atherosclerosis development in diet-induced hypercholesterolemia in mice, J. Nutr. Biochem. 23 (2012) 469–477.
[44] C.A. Thaiss, S. Itav, D. Rothschild, et al., Persistent microbiome alterations modulate the rate of post-dieting weight regain, Nature 450 (2016) 544–551.
[45] B. He, K. Nohara, N. Park, et al., The small molecule nobiletin targets the molecular oscillator to enhance circadian rhythms and protect against metabolic syndrome, Cell Metabol. 23 (2016) 610–621.